Catalysis Today xxx (2015) xxx–xxx

Contents lists available at ScienceDirect

Catalysis Today

journal homepage: www.elsevier.com/locate/cattod

Evaluation of Rh/$Ce_xTi_{1-x}O_2$ catalysts for synthesis of oxygenates from syngas using XPS and TPR techniques

Ephraim Sheerin, Gunugunuri K. Reddy, Panagiotis Smirniotis*

Chemical Engineering Program, Biomedical, Chemical & Environmental Engineering Department, University of Cincinnati, Cincinnati, OH 45221-0012, United States

ARTICLE INFO

Article history:
Received 13 April 2015
Received in revised form 16 July 2015
Accepted 30 July 2015
Available online xxx

Keywords:
Syngas
Ethanol
Methanol
Rhodium
Ce–Ti
Solid solutions
XPS
TPR

ABSTRACT

Rh/$Ce_xTi_{1-x}O_2$ catalysts have been investigated for the synthesis of ethanol from syngas. For this purpose various $Ce_xTi_{1-x}O_2$ (x = 0, 0.25, 0.5, 0.75, and 1) solid solution supports were synthesized using co-precipitation, which is an inexpensive and environmental friendly method. 2 wt% Rh has been deposited over these supports by using wet impregnation method. We have evaluated these Rh catalysts for synthesis of ethanol from syngas at atmospheric pressure and 350 psi. Among, the various catalysts, Rh supported on $Ce_{0.75}Ti_{0.25}O_2$ catalyst exhibit better selectivity toward oxygenates compared to other catalysts. Interestingly, Ti rich samples exhibit higher selectivity toward hydrocarbons while Ce rich samples exhibit higher selectivity toward oxygenated products. The catalytic results at atmospheric pressure show that titania rich catalysts exhibit higher H_2 conversion and ceria rich catalysts exhibit higher CO-conversion at 250 °C at atmospheric pressure. Temperature programmed reduction measurements suggest that Rh promotes the cerium surface reduction. X-ray photoelectron measurements show that all the catalysts exhibit peaks due to Ce^{4+} and Ce^{3+} oxidations states in the Ce 3d spectra. O1s spectra of activated Rh/TiO_2 and Rh/$Ce_{0.5}Ti_{0.5}O_2$ catalysts show two peaks after reduction in hydrogen. One peak is due to the oxygen atoms from the individual oxides and the other peak is from the compound formation between Rh and the support. X-ray photoelectron measurements of activated catalysts also show that Rh/$Ce_{0.5}Ti_{0.5}O_2$ catalyst exhibit higher Rh^{1+} ions on the surface compared to Rh/TiO_2 and exhibits better selectivity toward oxygenated products.

1. Introduction

Oxygenated carbon products like ethanol and methanol are very promising fuel alternatives and have attracted significant attention in recent years. Ethanol and Methanol are also one of the important starting feedstock for other chemicals production [1]. Methanol is produced in quantities over 50 million tons per year [2] and is present in many industrial sectors. It is used as a raw material for the synthesis of formaldehyde, one of the most important organic molecules (around 5×10^7 tons of formaldehyde produced per year) [3], for the synthesis of olefins [4,5], such as propylene and ethylene (bio polymer precursors). Ethanol is widely blended into the unleaded gasoline pool with varied percentages to significantly decreasing the dependence of our society on crude oil, at the same time reducing the harmful tailpipe emissions of CO, particulate matter, NO_x, and other pollutants. In fact, over two billion gallons of ethanol were produced in the US in 2002, mostly for use as a fuel additive [6]. Although this is small fraction of the US consumption of 134 billion gallons per year of gasoline, studies show that there is a potential to increase ethanol production to 34–75 billion gallons per year [7]. In addition to its potential application as a transportation fuel, bioethanol has been considered as a feedstock for the synthesis of variety of chemicals, fuels, and polymers. Methanol is also known as a fuel [4,8–10] either for fuel cells [11] or mixed with gasoline, or indirectly as a raw material for the synthesis of diesel, gasoline, dimethylether, hydrocarbons. Thus, the synthesis of oxygenated products like methanol, and ethanol allows getting stable and easily stored energy, as alternatives to fossil fuels. As fuels, ethanol and methanol have several ideal properties: they are nontoxic, easy to store and also transportation fuel results in lower net petroleum use and lower green house gas emissions than gasoline per mile driven. Consequently, there is a growing worldwide interest in the production of oxygenates from biomass and possibly from other readily available carbonaceous sources such as coal without CO_2 emission, and its use as a fuel for transportation, chemical feed stocks, and as an hydrogen carrier in the future.

---

* Corresponding author.
E-mail addresses: smirnipp@ucmail.uc.edu, Panagiotis.Smirniotis@uc.edu (P. Smirniotis).

http://dx.doi.org/10.1016/j.cattod.2015.07.050
0920-5861/

The catalysts for the synthesis of oxygenates from syngas can be classified into four categories: (a) Rh based catalysts [12], (b) Cu based catalysts [13], (c) modified Fisher–Tropsch catalysts [14,15], (d) modified Mo-based catalysts [16]. Among the various catalysts, Rh-based catalysts received much attention because of its high activity and its ability to adsorb reactive CO both associatively and dissociatively, allowing it to form both hydrocarbons and oxygenates [12]. Because Rh is an expensive metal, the improvement of activity and ethanol selectivity over Rh-based catalysts is necessary for achieving a commercial available process.

The mechanism of the syngas to various products over Rh based catalysts was proposed by the Arakawa et al. [16]. The main products of the reaction are hydrocarbons, oxygenates, and CO_2. According to their mechanism, first CO and H_2 adsorbs on the Rh^0 site [16]. Then, hydrogen dissociates into adsorbed hydrogen (H_{ad}). Some of the CO dissociates into carbon and atomic oxygen. Then, H_{ad} combines with C and started to form CH_x fragments. Combination of two or three CH_x fragments or addition of more H_{ad} to the CH_x fragment leads to the formation of hydrocarbons like methane, ethane, propane, etc. This reaction primarily happens on metallic Rh sites. On the other hand insertion of CO into the CH_x fragments leads to the formation of CH_2CO, CH_3CO fragments which finally are converted or rearranged into oxygenates. The insertion of CO into CH_x fragment occurs on Rh^{1+} site. Hence, the mechanism suggest that metallic Rh is mainly responsible for the CO and H_2 conversion and Rh^{1+} is responsible for the oxygenated product formation. Hence, it is important to have balance between Rh^0 and Rh^{1+} ions to have better oxygenated products yield.

The influence of various promoters on the catalytic activity of Rh has been extensively studied in recent years. Metal catalysts supported on reducible metal oxides exhibit remarkably enhanced performance in many catalytic processes, including hydrogenation [17], partial oxidation [18], or reforming reaction [19]. A strong interaction between support and metal (SMSI) exists in the CeO_2-supported metal catalysts and gives the catalysts with high activity for many catalytic reactions [20–22]. However, the main problem associated with the ceria is poor thermal stability and low lattice oxygen vacancies [23]. On the other hand, lattice oxygen of the support is very important for the SMSI interactions. Introduction of metal ions into the CeO_2 lattices improves the oxygen vacancies and catalytic performance of CeO_2-supported metal catalysts through changing the physical and chemical properties of the supports [24–26].

In the present study, we investigated the catalytic performance of $Rh/Ce_xTi_{1-x}O_2$ catalysts for the synthesis of oxygenates from syngas. Our XPS measurements show that $Ce_xTi_{1-x}O_2$ mixed oxides exhibits higher Rh^{1+} ions on the surface and exhibit better selectivity toward oxygenated products. Our catalytic measurements at atmospheric pressure show that CeO_2 and $Ce_{0.75}Ti_{0.25}O_2$ catalysts exhibits higher CO conversion and TiO_2 and $Ti_{0.75}Ce_{0.25}O_2$ catalysts exhibit higher CO conversion. Among the various catalysts $Rh/Ce_{0.75}Ti_{0.25}O_2$ catalyst exhibits best selectivity toward oxygenated products.

2. Experimental

2.1. Catalyst synthesis

2.1.1. Preparation of $Ce_xTi_{1-x}O_2$ supports

Various $Ce_xTi_{1-x}O_2$ ($x = 0$–1) supports were prepared by using co-precipitation method. In a typical preparation, calculated amounts of ammonium cerium nitrate and titanium chloride are dissolved separately in deionized water and the aqueous solutions mixed. Dilute aqueous ammonia was added gradually drop wise to the mixture solutions, and vigorously stirred; until precipitation was complete (pH ≈ 8.5). The obtained precipitate gels were further aged overnight, and filtered off. The obtained cakes were oven dried at 80 °C for 12 h, and finally calcined at 500 °C for 5 h. The rate of heating as well as cooling was kept at 5 °C min^{-1}.

2.1.2. Preparation of $Rh/Ce_xTi_{1-x}O_2$ catalysts

The $Rh/Ce_xTi_{1-x}O_2$ catalysts are synthesized by using wet impregnation method. In a typical synthesis, 50 mL of deionized water was added to a 100 mL beaker containing 1.0 g of support. The mixture was heated to 80 °C, under continuous stirring conditions. A predetermined quantity of rhodium nitrate precursor was then added, and the mixture was evaporated to dryness. The resulting material obtained was further dried overnight at 110 °C. Finally, the catalyst was calcined at 450 °C for 5 h.

2.2. Catalyst characterization

2.2.1. BET surface area analysis

The BET surface areas were obtained by N_2 adsorption on a Micromeritics ASAP 2010 Instrument. Prior to the analysis, samples were oven dried at 120 °C for 12 h and flushed with Argon for 2 h. The pore size distribution analyses were conducted by N_2 physisorption at liquid N_2 temperature using Micromeritics ASAP 2010 apparatus. All samples were degassed at 300 °C under vacuum before analysis.

2.2.2. X-ray diffraction measurements

Powder X-ray diffraction (XRD) patterns were recorded on a Phillips Xpert diffractometer using nickel-filtered Cu Kα (0.154056 nm) radiation source. 0–80 °C were collected using 0.02 step size and a counting time of 1 s per point. Crystalline phases were identified by comparing the observed reflections with the reference ones from ICDD files [27].

2.2.3. TPR measurements

The temperature-programmed reduction (TPR) with hydrogen, of various catalyst samples were performed by means of an automated catalyst characterization system (Micromeritics, model AutoChem II 2920), which incorporates a thermal conductivity detector (TCD). The experiments were carried out at a heating rate of 5 °C min^{-1}. The reactive gas composition was H_2 (10 vol.%) in nitrogen. The flow rate was fixed at 10 mL/min (STP). The TPR measurements were carried out following activation after cooling the sample in helium flow to 50 °C. The sample was then held at 50 °C under flowing helium to remove the remaining adsorbed oxygen until the TCD signal returned to the baseline. Subsequently, the TPR experiments were performed up to a temperature of 800 °C. The water formed during the reduction was removed by using an ice trapper. The gas stream coming from the reactor was passed through a trapper before the gas entered into the G.C. A mixture of isopropanol and liquid nitrogen was used in the trapper to remove the formed water during the TPR experiment.

2.2.4. Raman spectroscopy measurements

The Raman spectra of all the samples investigated in the present study were obtained on HORIBA Jobin Yvon HR 800 equipped with a liquid-nitrogen cooled CCD detector. The emission line at 514.5 nm from Ar^+ ion laser was focused on the sample under microscope and the analyzed spot being ∼1 μm. The power of the incident beam on the sample was 3 mW. Time of acquisition was adjusted according to the intensity of the Raman scattering. The wavenumber values reported from the spectra are accurate to within 2 cm^{-1}.

2.2.5. XPS measurements

The X-ray photoelectron spectroscopy (XPS) measurements were performed on a Pyris VG Thermo Scientific spectrometer using

Please cite this article in press as: E. Sheerin, et al., Evaluation of $Rh/Ce_xTi_{1-x}O_2$ catalysts for synthesis of oxygenates from syngas using XPS and TPR techniques, Catal. Today (2015), http://dx.doi.org/10.1016/j.cattod.2015.07.050

Al Kα (1486.6 eV) radiation as the excitation radiation. Charging of the catalyst samples was corrected by setting the binding energy of the adventitious carbon (C 1s) at 284.6 eV. The XPS analysis was performed at ambient temperature and at pressures typically on the order of $<10^{-8}$ Torr [28]. Prior to analysis, the samples were out gassed under vacuum for 4 h. The Rh 3d spectra of activated catalysts were deconvulated to deduce the Rh^{1+}/Rh^0 on the surface.

2.3. Catalytic activity

2.3.1. High pressure experiments

The syngas to ethanol reaction was carried out in a vertical down flow fixed bed differential stainless steel reactor at 350 psi. In a typical experiment, ca. required amount of powdered catalyst was placed between two plugs of quartz wool. The reactor is filled with glass beads below and above the catalyst to avoid the free space. The reactor was placed vertically inside a programmable tubular furnace (Lindberg), which was heated electrically. The pressure of the reactor was maintained by the back pressure regulators. Before the reaction the catalyst was reduced at 300 °C in the presence of hydrogen for 2 h. After the reduction, the temperature of the reactor was bought to the desired temperature and the H_2/CO mixture ($H_2/CO = 2$) was introduced into the reactor. The products of the reactions were analyzed using HP gas chromatograph. The CO conversion was calculated by

$$X_{CO}(\%) = \frac{CO_f - CO_i}{CO_i} \times 100$$

The selectivity of products were calculated by

$$S_{EtOH}(\%) = \frac{n_i C_i}{\sum n_i C_i} \times 100$$

The yield of oxygenates was calculated by

$$\frac{Y_{oxy} = X_{co}(\%) \times S_{oxy}(\%)}{10,000}$$

2.3.2. Experiments at atmospheric pressure

The syngas to ethanol reaction was carried out in a vertical down flow fixed bed quartz reactor with 6 mm i.d. at atmospheric pressure. In a typical experiment, ca. required amount of powdered catalyst was placed between two plugs of quartz wool. The reactor was placed vertically inside a programmable tubular furnace, which was heated electrically. Before the reaction the catalyst was reduced at 300 °C in the presence of hydrogen for 2 h. After the reduction, the temperature of the rector bought to desired temperature and the H_2/CO mixture ($H_2/CO = 2$) was introduced into the reactor.

3. Results and discussion

3.1. Catalytic activity

3.1.1. Experiments at atmospheric pressure

Initially, we have evaluated $Rh/Ce_xTi_{1-x}O_2$ catalysts for syngas to oxygenates synthesis at atmospheric pressure to investigate the effect of the support on the catalytic properties of Rh. It is known that the structural and catalytic properties of the CeO_2, TiO_2 and Ce–Ti mixed oxides are completely different. It is very important to investigate the adsorption behavior of CO and H_2 over these mixed oxides. At atmospheric pressure the reaction between CO and H_2 is very simple and methane and CO_2 are the main products and hence, we can understand the catalysts behavior easily. We have evaluated all the catalysts at two temperatures namely, 250 °C and 300 °C. The hydrogen conversion, and CO conversion are presented in Figs. 1 and 2, respectively. Interestingly, hydrogen conversion increases with increasing the amount of titania amount into the cerium lattice. The order of activity is $Rh/TiO_2 > Rh/i_{0.75}Ce_{0.25}O_2 > Rh/Ti_{0.5}Ce_{0.5}O_2 > Rh/Ti_{0.25}Ce_{0.75}O_2 > Rh/CeO_2$. On the other hand, the CO conversion decreases with increasing the amount of titania into the cerium lattice at 250 °C. The order of activity is $Rh/Ti_{0.25}Ce_{0.75}O_2 > Rh/Ti_{0.75}Ce_{0.25}O_2 > Rh/Ti_{0.5}Ce_{0.5}O_2 \ggg Rh/CeO_2 > Rh/TiO_2$. CeO_2 favors CO dissociation and the TiO_2 favors hydrogen dissociation. These results clearly show that hydrogen decomposes at the Rh–TiO_x interface and CO decomposes at Rh–CeO_x interface. Interestingly, at atmospheric pressure only products with single carbon like CH_4, CO_2, CH_3OH were observed. There is no formation of products with higher number of carbons like ethanol, acetaldehyde, or ethane, etc. Since hydrogen conversion is high for titania rich samples, these samples also exhibited better yields toward CH_4, CO_2, CH_3OH, and H_2O.

Completely different behavior observed at reaction temperature 300 °C. Only Rh/TiO_2 and $Rh/Ti_{0.25}Ce_{0.75}O_2$ catalysts exhibited higher catalytic activity. Rh/CeO_2 and $Rh/Ce_{0.5}Ti_{0.5}O_2$ catalysts exhibited least activity. Even though the $Rh/Ce_{0.25}Ti_{0.75}O_2$ catalyst initially exhibited higher activity, however it deactivates with time. Both Rh/TiO_2 and $Rh/Ti_{0.25}Ce_{0.75}O_2$ exhibited similar hydrogen conversions of about 80–85%. The order of hydrogen conversion is $Rh/TiO_2 > Rh/Ti_{0.25}Ce_{0.75}O_2 > Rh/Ti_{0.75}Ce_{0.25}O_2 > Rh/Ti_{0.5}Ce_{0.5}O_2 > Rh/CeO_2$. Interestingly, $Rh/Ti_{0.25}Ce_{0.75}O_2$ catalyst exhibited much higher CO conversion compared to Rh/TiO_2 catalyst. These results confirm that presence of ceria favors the CO dissociation. $Rh/Ti_{0.25}Ce_{0.75}O_2$ catalyst exhibited CO conversion of 40% and Rh/TiO_2 exhibited CO conversion below 10%. The, Rh/TiO_2 catalyst exhibited lesser CO conversion than $Rh/Ti_{0.25}Ce_{0.75}O_2$ and $Rh/Ti_{0.5}Ce_{0.5}O_2$ catalysts. The order of activity of CO conversion is $Rh/Ti_{0.75}Ce_{0.25}O_2 > Rh/Ti_{0.25}Ce_{0.75}O_2 > Rh/Ti_{0.5}Ce_{0.5}O_2 > Rh/TiO_2 > Rh/CeO_2$. Both Rh/TiO_2 and $Rh/Ti_{0.25}Ce_{0.75}O_2$ catalysts exhibited similar yield toward CO_2. However, $Rh/Ti_{0.25}Ce_{0.75}O_2$ catalysts exhibited much higher yield toward methanol compared to the Rh/TiO_2 catalyst. Moreover, Rh/TiO_2 catalyst exhibited much higher CH_4 yield compared to the $Rh/Ti_{0.25}Ce_{0.75}O_2$ catalyst. These results show that CeO_2 favors oxygenated product formation and TiO_2 favors hydrocarbon product formation at atmospheric pressure.

3.1.2. Experiments at 350 psi pressure

The five catalysts consist of 2% Rh (wt%) loaded on pure ceria, pure titania, and mixed metal oxides, Rh/CeO_2, Rh/TiO_2, $Rh/Ce_xTi_{1-x}O_2$. Fig. 3 shows the CO conversion profiles of various $Rh/Ce_xTi_{1-x}O_2$ catalysts as a function of reaction temperature. The catalysts Rh/TiO_2, Rh/CeO_2 and $Rh/Ce_{0.5}Ti_{0.5}O_2$ exhibit 100% CO conversion at 325 °C. Between Rh/CeO_2 and Rh/TiO_2 catalysts, the titania supported catalyst exhibits higher CO conversion.

We divided all the products into three categories, namely hydrocarbon, oxygenated and CO_2 products. The selectivities of hydrocarbon, oxygenated and CO_2 products for various Rh/TiO_2, Rh/CeO_2 and $Rh/Ce_xTi_{1-x}O_2$ catalysts are presented in Table 1. Since all the catalysts exhibit very low conversions at 250 and 275 °C, the selectivites are presented for only for 300 °C and 325 °C reaction temperatures. All tested catalysts formed carbon dioxide during the reaction with atomic carbon selectivities between 1 and 16% from 225 °C to 325 °C. As shown in Table 1, Ce rich samples shows lower selectivity toward CO_2 and Ti rich samples shows higher selectivity toward CO_2. Also, Ce rich compounds exhibit higher selectivities toward oxygenated products and lower selectivity toward hydrocarbon products. Ti rich catalysts exhibit lower selectivities toward oxygenated products and higher selectivity toward hydrocarbon products. Among the various catalysts, the $Rh/Ce_{0.75}Ti_{0.25}O_2$ exhibits better selectivity and yield toward oxygenated products.

Please cite this article in press as: E. Sheerin, et al., Evaluation of $Rh/Ce_xTi_{1-x}O_2$ catalysts for synthesis of oxygenates from syngas using XPS and TPR techniques, Catal. Today (2015), http://dx.doi.org/10.1016/j.cattod.2015.07.050

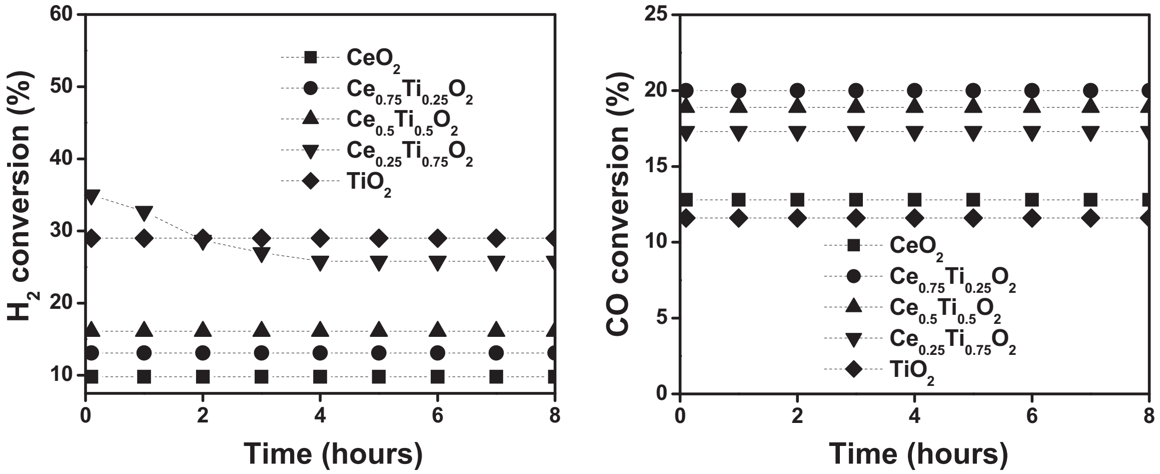

Fig. 1. H_2 and CO conversion over various Rh/$Ce_xTi_{1-x}O_2$ (x = 0–1) catalysts (temperature: 250 °C, pressure: 1 atm, H_2/CO = 2, space velocity 12,000 mL $g_{cat}{}^{-1}$ h^{-1}).

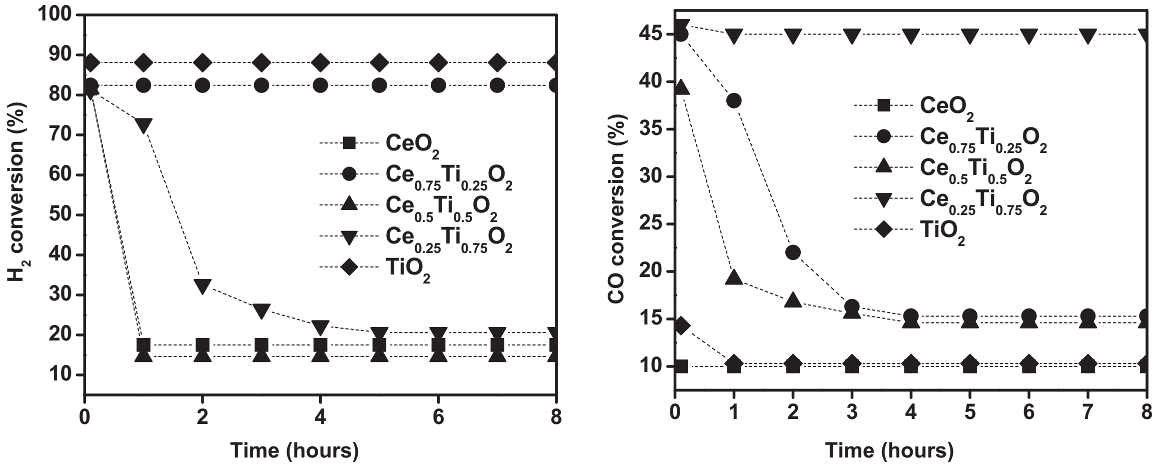

Fig. 2. H_2 and CO conversion over various Rh/$Ce_xTi_{1-x}O_2$ (x = 0–1) catalysts (temperature: 300 °C, pressure 1 atm, H_2/CO = 2, space velocity 12,000 mL $g_{cat}{}^{-1}$ h^{-1}).

Rh supported on $Ce_{0.75}Ti_{0.25}O_2$ catalyst (0.60) exhibits better oxygenated yields compared to the Rh/CeO_2 (0.58) and Rh/TiO_2 (0.51) catalysts at 300 °C. Rh catalysts loaded on pure oxide supports result in less oxygenated yield than the mixed oxide supported catalysts. Even though Rh/TiO_2 exhibited higher CO conversion compared to some of the mixed oxide supports, it exhibits lowest selectivity toward ethanol compared to mixed oxide supports. Interestingly, Ti rich supports exhibit higher selectivity toward hydrocarbons and Ce rich supports exhibit higher selectivity toward oxygenated products.

3.2. *Catalyst characterization*

3.2.1. *BET specific surface area*

BET surface areas are presented in Table 2. Pure titania has a measured surface area of 94 m^2/g, and pure ceria has a measured

Table 1
CO conversion, CO_2 selectivity, oxygenated selectivity, hydrocarbon selectivities of various Rh/TiO_2, Rh/CeO_2 and Rh/$Ce_xTi_{1-x}O_2$ catalysts (H_2/CO = 2, pressure = 350 psi, 2 wt% Rhodium, space velocity 6000 mL $g_{cat}{}^{-1}$ h^{-1}, oxygenated selectivity: methanol + ethanol + propanol + acetaldehyde + formaldehyde + formic acid, hydro carbon selectivity: methane + ethane + propane).

Catalyst		CO_2 selectivity	Ethanol selectivity	Oxygenated selectivity	Hydrocarbon selectivity
Rh/CeO_2	300 °C	52.9	10.3	44.4	52.9
	325 °C	59.1	6.8	35.2	59.1
Rh/$Ce_{0.75}Ti_{0.25}O_2$	300 °C	33	15.1	54.3	33
	325 °C	48.9	4.4	35.3	48.9
Rh/$Ce_{0.5}Ti_{0.5}O_2$	300 °C	56.1	10.8	34.9	56.1
	325 °C	62.4	4	19.7	62.4
Rh/$Ce_{0.25}Ti_{0.75}O_2$	300 °C	65	1	13	65
	325 °C	67.3	0.3	10.1	67.3
Rh/TiO_2	300 °C	77.7	3.2	15	77.7
	325 °C	80.8	2.1	10.7	80.8

Please cite this article in press as: E. Sheerin, et al., Evaluation of Rh/$Ce_xTi_{1-x}O_2$ catalysts for synthesis of oxygenates from syngas using XPS and TPR techniques, Catal. Today (2015), http://dx.doi.org/10.1016/j.cattod.2015.07.050

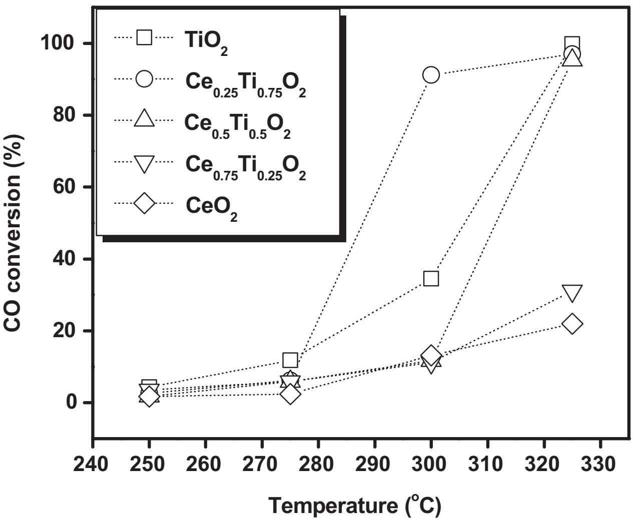

Fig. 3. CO conversion of Rh/$Ce_xTi_{1-x}O_2$ (x = 0–1) catalysts at various temperatures (H_2/CO = 2, pressure = 350 psi, 2 wt% rhodium, space velocity 6000 mL g_{cat}^{-1} h^{-1}).

Table 2
BET surface areas of pure supports and Rh promoted catalysts.

	SSA[a]	Rh loading[b]	SSA[a]
CeO_2	57	Rh/CeO_2	67
TiO_2–CeO_2 (1:3)	143	Rh/TiO_2–CeO_2 (1:3)	122
TiO_2–CeO_2 (1:1)	176	Rh/TiO_2–CeO_2 (1:1)	134
TiO_2–CeO_2 (3:1)	208	Rh/TiO_2–CeO_2 (3:1)	173
TiO_2	94	Rh/TiO_2	67

[a] Measured by N2 absorption method.
[b] BET surface area after Rh loading.

surface area of 57 m^2/g. The incorporation of titania into the ceria lattice increases the support surface area by more than double. Among the various supports, $Ce_{0.25}Ti_{0.75}O_2$ catalyst exhibits the highest surface area of 208 m^2/g. The increase in the surface area is due to incorporation of Ti into the ceria lattice and formation of solid solution [25]. There is a slight surface area decrease for all the supports after impregnating with Rh; this is possibly due to pore-blocking of the support by Rh.

3.2.2. X-ray diffraction (XRD)

The X-ray diffraction patterns of pure supports and Rh promoted samples are presented in Figs. 4 and 5. Pure Ceria exhibits peaks at 28.4°, 33.1°, 47.3°, 56.3°, 69.5° 2θ values. These peaks are due to the cubic fluorite structure of ceria. Similarly the X-ray diffraction pattern of the titania exhibits peaks due to the anatase phase which is active for catalytic applications compared to the titania rutile phase. Interestingly, there are no peaks corresponding to titania rutile phase. All the Ce–Ti mixed oxides exhibit amorphous patterns. This is mainly due to the formation of mixed metal oxides and decrease in the crystallite size [27]. The X-ray diffraction patterns of the Rh promoted ceria and titania catalysts also exhibit peaks due to the cubic fluorite structure of ceria and titania anatase phase, respectively. All the mixed oxide Rh catalysts exhibit amorphous patterns due to the high specific surface area and the formation of Ce–Ti solid solutions.

3.2.3. Raman spectroscopy

The Raman spectra of pure supports are shown in Fig. 6. Raman spectroscopy results are consistent with X-ray diffraction measurements. The Raman spectra of CeO_2 show a peak around 465 cm^{-1}, which is due to the cubic fluorite structure of ceria [23]. Titania exhibits peaks due to the titania-anatase phase, and again there

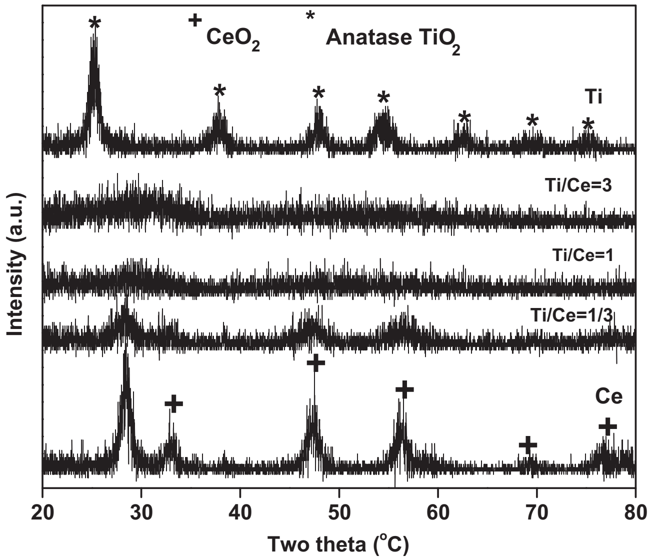

Fig. 4. X-ray diffraction profiles of various $Ce_xTi_{1-x}O_2$ supports.

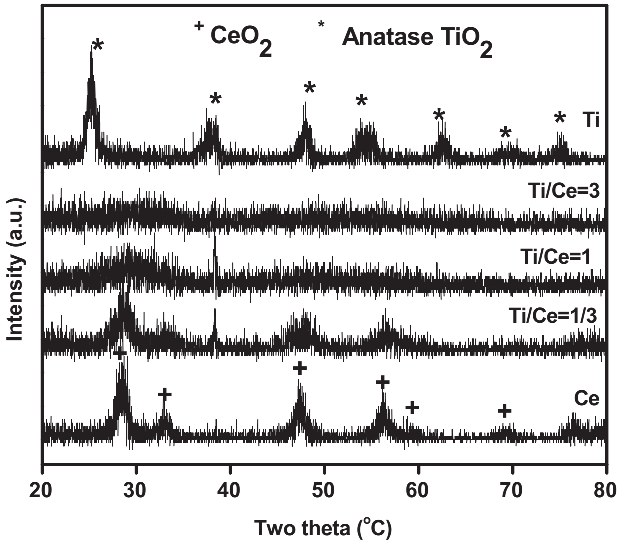

Fig. 5. X-ray diffraction profiles of various Rh/$Ce_xTi_{1-x}O_2$ supports.

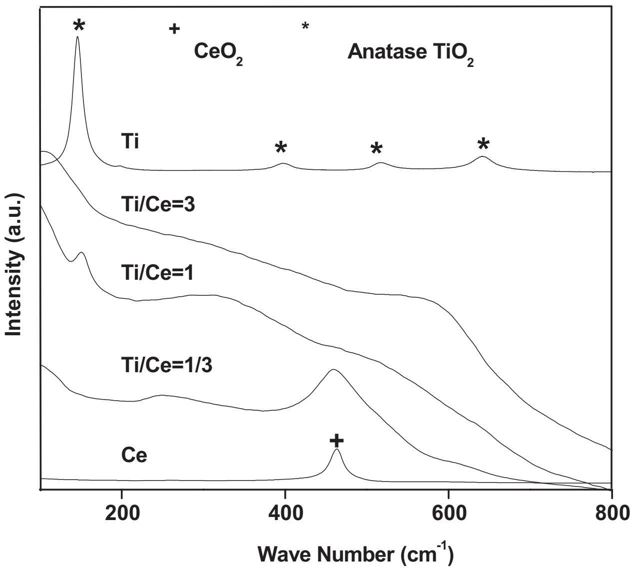

Fig. 6. Raman spectra of various Rh/$Ce_xTi_{1-x}O_2$ supports.

Please cite this article in press as: E. Sheerin, et al., Evaluation of Rh/$Ce_xTi_{1-x}O_2$ catalysts for synthesis of oxygenates from syngas using XPS and TPR techniques, Catal. Today (2015), http://dx.doi.org/10.1016/j.cattod.2015.07.050

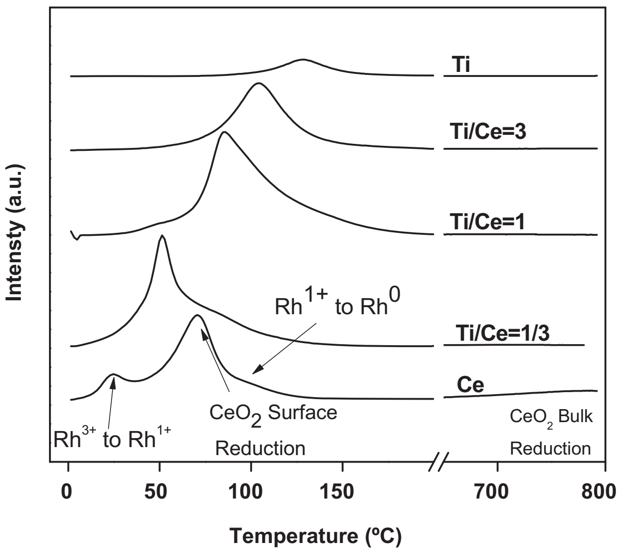

Fig. 7. Temperature programmed reduction profiles of various Rh/Ce$_x$Ti$_{1-x}$O$_2$ supports.

are no peaks corresponding to the titania-rutile phase. The Raman spectra of mixed oxide show amorphous patterns, which is consistent with XRD patterns. There are no peaks corresponding to Rh oxide or compounds between Rh oxide and support, which suggest that Rh is in highly dispersed state over the ceria-titania supports (not shown).

3.2.4. TPR

The TPR profiles of the various Rh promoted catalysts are presented in Fig. 7. The TPR profile of the Rh/CeO$_2$ catalyst exhibits a total of four reduction peaks. The peak at 25 °C corresponds to the reduction of Rh^{3+} to Rh^{1+}. The other two peaks at around 75 °C are due to the reduction of Rh^{1+} to Rh metal and ceria surface reduction. The peak at higher temperature is due to the ceria bulk reduction. As per literature reports, the surface ceria reduction occurs at 500 °C and bulk ceria reduction occurs at 800 °C in the case of pristine ceria sample [29]. However, in the present study, the ceria surface reduction occurs at 75 °C. This is due to the strong metal support interaction (SMSI) between Rh and ceria, which indicates high catalytic activity. Moreover, the deposition of noble metals on ceria-based materials strongly enhances the reducibility of Ce^{4+} due to hydrogen spillover on the surface. The surface oxygen vacancies were introduced by hydrogen spillover from the noble metal to the catalyst support, and then these vacancies at the surface were subsequently filled up by the bulk oxygen being transported to the surface due to ionic conductivity. The TPR pattern of Rh/Ce$_{0.75}$Ti$_{0.25}$O$_2$ sample exhibits different pattern compared to Rh/CeO$_2$ sample. In this case, Rh^{3+} to Rh^{1+} reduction and the surface ceria reduction occurs simultaneously, and then reduction due to Rh^{1+} to Rh^0. The reduction temperature of all the three peaks shifted to lower temperature compared to Rh/CeO$_2$. This is due to the incorporation of titania, into the ceria lattice. The defect throughout the crystal produced an increase in the oxygen mobility and diffusion in the lattices, which promotes the reduction of both surface and bulk reductions in the CeO$_2$–TiO$_2$ supports. This type of behavior was well reported in the literature. The reduction behavior of ceria depends on several parameters like synthesis method, type of metal ion doped, crystallite size, etc. The TPR patterns of Rh/Ce$_{0.5}$Ti$_{0.5}$O$_2$ and Rh/Ce$_{0.25}$Ti$_{0.75}$O$_2$ are similar. For both catalysts exhibited peaks due to Rh^{3+} to Rh^{1+} reduction, Rh^{1+} to Rh^0 reduction, and ceria surface reduction happened simultaneously. Interestingly, in these supports the reduction temperatures once again shifted to higher temperatures. EDX analysis was performed on all the catalysts to find out the atomic composition of the catalyst. The adjusted weight and atomic % of various components in various catalysts are presented Table 3. All the catalysts exhibit atomic percentages according to compositions within the experimental error.

Table 3
Atomic percentages of various components in Rh/Ce$_x$Ti$_{1-x}$O$_2$ catalysts determined EDX.

	Weight %				Atomic %			
	Rh	Ti	Ce	O	Rh	Ti	Ce	O
CeO$_2$	5.2		80	15	3.54		32.2	64.3
TiO$_2$–CeO$_2$ (1:3)	2.7	6.8	72.4	18	1.5	8.3	24.5	65.7
TiO$_2$–CeO$_2$ (1:1)	4.8	16	5.7	21.4	2.3	16.3	16.3	65.1
TiO$_2$–CeO$_2$ (3:1)	5.5	30	37.4	21.4	2.1	24.2	8.4	65.3
TiO$_2$	6	56.4		37.7	1.6	32.8		65.6

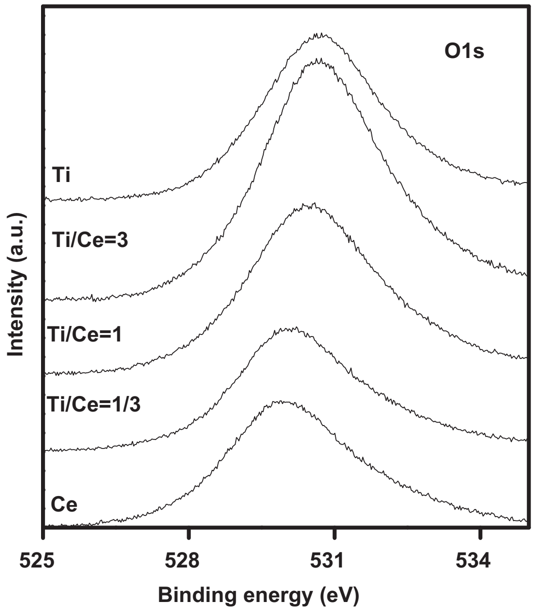

Fig. 8. O1s X-ray photoelectron spectra of various Rh/Ce$_x$Ti$_{1-x}$O$_2$ supports.

Table 4
XPS binding energies of various Rh/Ce$_x$Ti$_{1-x}$O$_2$ catalysts and Rh^{1+}/Rh^0 ratios of Rh/TiO$_2$ and Rh/Ce$_{0.5}$Ti$_{0.5}$O$_2$ catalysts.

	O 1s	Rh 3d	Ti 2p	Ce 3d
CeO$_2$	530	310.3		916.7
TiO$_2$–CeO$_2$ (1:3)	530.1	309.5	458.5	918.4
TiO$_2$–CeO$_2$ (1:1)	530.5	310.2	458.9	918.6
TiO$_2$–CeO$_2$ (3:1)	530.6	310	459.1	918.5
TiO$_2$	530.7	310.2	459.2	

3.2.5. X-ray photoelectron spectroscopy (XPS)

X-ray photoelectron measurements were performed over Rh/Ce$_x$Ti$_{1-x}$O$_2$ catalysts to investigate the surface properties and elemental oxidation states. Figs. 8–11 show the O1s, Rh 3d, Ti 2p, and Ce 3d spectra of Rh/Ce$_x$Ti$_{1-x}$O$_2$ catalysts. The binding energy values of O1s, Rh 3d, Ti 2p and Ce 3d of all the fresh catalysts are presented in Table 4. The O1s peak is generally broad and complicated, because of the nonequivalence of surface O ions from different oxides. As per the literature, the O ions in pure CeO$_2$ exhibit intense peaks at 529.6 eV. The O 1 s binding energy values reported for TiO$_2$ are 530.0 eV, respectively [28]. All the samples exhibit only one peak around 530 eV. This peak is due to the ionization of oxygen atom from support. As expected, the O1s peak shifted

Please cite this article in press as: E. Sheerin, et al., Evaluation of Rh/Ce$_x$Ti$_{1-x}$O$_2$ catalysts for synthesis of oxygenates from syngas using XPS and TPR techniques, Catal. Today (2015), http://dx.doi.org/10.1016/j.cattod.2015.07.050

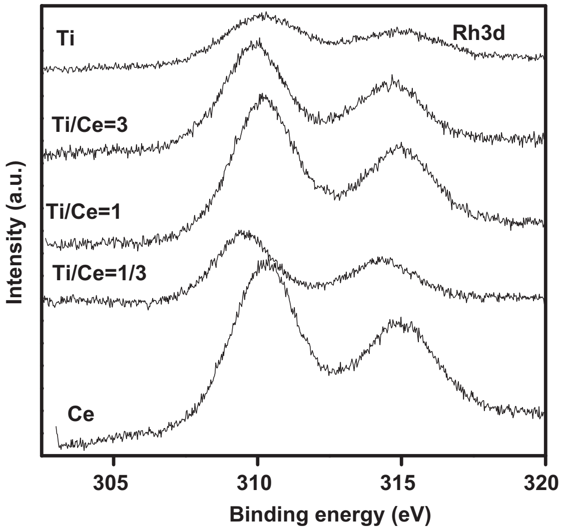

Fig. 9. Rh 3d X-ray photoelectron spectra of various Rh/$Ce_xTi_{1-x}O_2$ supports.

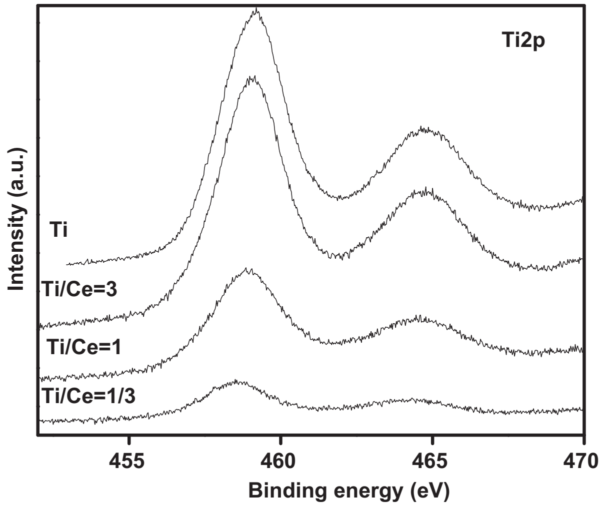

Fig. 10. Ti 2p X-ray photoelectron spectra of various Rh/$Ce_xTi_{1-x}O_2$ supports.

to higher binding energy side from Ce-rich samples to Ti-rich samples.

Rh 3d XPS spectra of various Rh/$Ce_xTi_{1-x}O_2$ catalysts are presented in Fig. 9. All the samples exhibit a peak around 310 eV along with a satellite at 315 eV. These peaks primarily belong to Rh^{3+} oxidation state. These results confirm the formation of Rh_2O_3 during the impregnation of Rh over ceria-titania mixed oxides. Fig. 10 also shows Ti 2p XPS spectra of the various Ti samples investigated in the present study. All the samples exhibit a peak at around 458 eV with

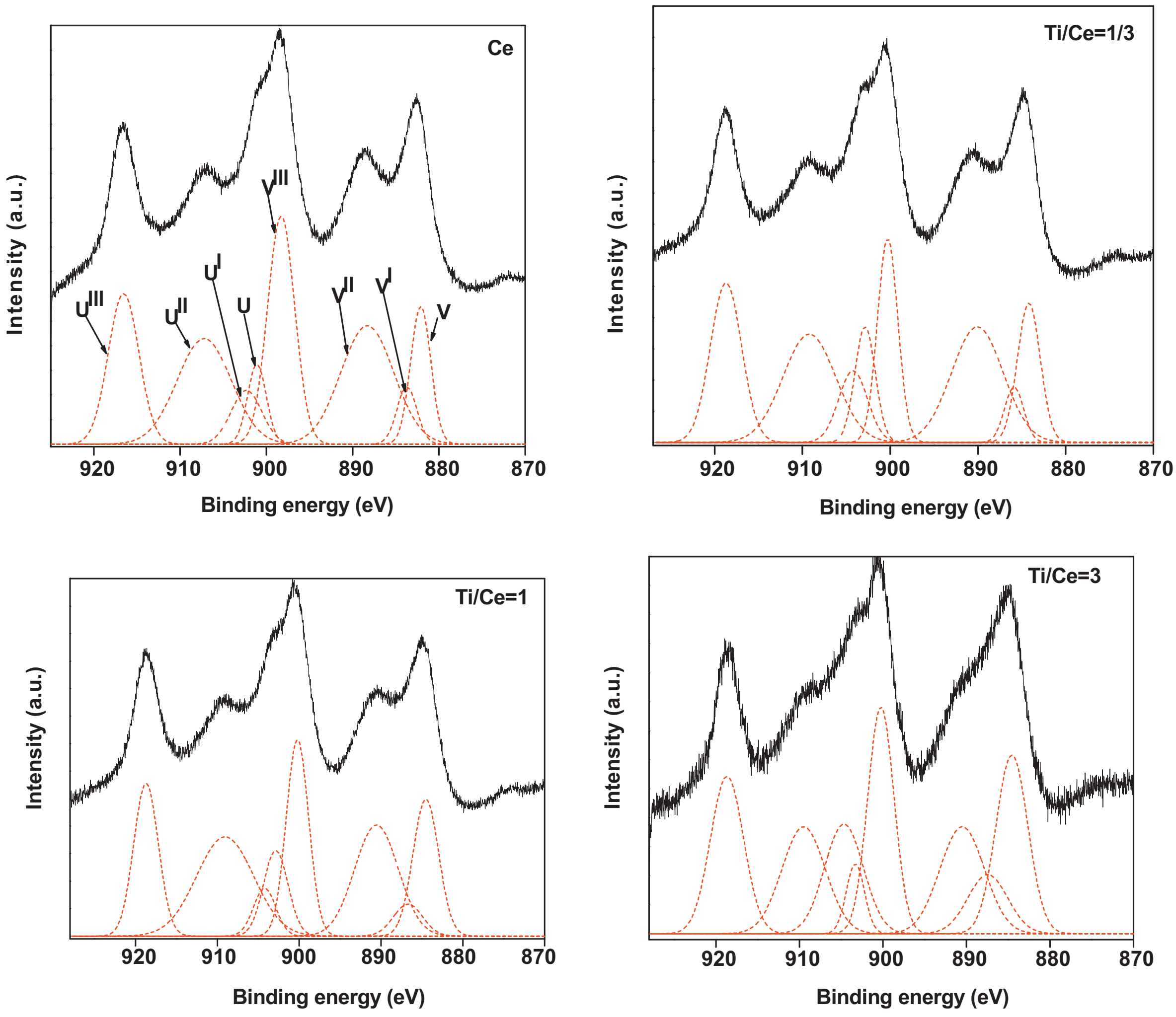

Fig. 11. Ce 3d X-ray photoelectron spectra of various Rh/$Ce_xTi_{1-x}O_2$ supports.

Please cite this article in press as: E. Sheerin, et al., Evaluation of Rh/$Ce_xTi_{1-x}O_2$ catalysts for synthesis of oxygenates from syngas using XPS and TPR techniques, Catal. Today (2015), http://dx.doi.org/10.1016/j.cattod.2015.07.050

a satellite at 465 eV. These results suggest that Ti is in 4+ oxidation state.

The Ce 3d XPS spectra of Rh//$Ce_xTi_{1-x}O_2$ catalysts are presented in Fig. 11. Typically, the Ce 3d XPS core level spectra exhibit three lobed envelopes (around 879–890, 895–910, and 916 eV) such as those ionization, depicted in Fig. 11. From these envelopes, the coexistence of both Ce^{3+} and Ce^{4+} oxidation states is distinguishable, although the 4+ oxidation state is predominant. The bands labeled "v" collectively represent the Ce $3d_{5/2}$ ionization, while bands labeled "u" represent the Ce $3d_{3/2}$ ionization [30]. The bands with unprimed labels represent the primary Ce $3d_{5/2}$ and Ce $3d_{3/2}$ transitions, while the primed labels represent ionization satellite features. Specifically, the band (u^0, u) is the Ce $3d_{3/2}$ ionization and the band (v^0, v) is the Ce $3d_{5/2}$ ionization for Ce^{3+} and Ce^{4+}. The bands labeled v', v'', v''' and u', u'', u''' are satellites arising from the Ce $3d_{5/2}$ ionization and Ce $3d_{3/2}$, respectively. According to Burroughs et al. (1976), the peaks u' and v' arise from Ce^{3+} oxidation state and remaining peaks arises from Ce^{4+} oxidation state. Interestingly, all the samples exhibit peaks due to both Ce^{3+} and Ce^{4+} oxidation states. Among the various samples $Rh/Ce_{0.25}Ti_{0.75}O_2$ catalysts sample exhibits higher intensity of Ce^{3+} peaks.

Our catalytic results show that the mixed oxides exhibit better selectivity toward oxygenates compared to the titania alone. We investigated by using XPS. Rh/TiO_2 and $Rh/Ce_{0.5}Ti_{0.5}O_2$ activated catalysts after reduction in hydrogen at 300 °C for 2 h The O1s, Rh 3d X-ray photoelectron spectra of Rh/TiO_2 and $Rh/Ce_{0.5}Ti_{0.5}O_2$ activated catalysts after reduction in hydrogen at 300 °C for 2 h are presented in Figs. 12 and 13, respectively. Interestingly, the activated Rh/TiO_2 and $Rh/Ce_{0.5}Ti_{0.5}O_2$ exhibit two peaks in the O1s XPS spectra. One peak is due to the oxygen atoms from the individual oxides and the other peak is from the compound formation between Rh and the support. During the reduction due to the strong metal support interaction there will be formation of partially reducible oxide compounds like Rh^{1+}–CeO_{2-x} and Rh^{1+}–TiO_{2-x}. The formation of these compounds is very important for the formations of Rh^{1+} species. Formation of these compounds stabilizes the Rh^{1+} species during the reaction. These results are in good agreement with the literature reports. Reddy et al. [31] reported that $V_2O_5/CeO_2/Al_2O_3$ exhibits an additional peak in the O1s spectra when there is a formation $CeVO_4$ compound along with regular peak. Another study also Ca/Zr sorbents synthesized by aerosol method exhibits two peaks in the O1s XPS spectra one due to individual oxides and other is due to formation of $CaZrO_3$ [32–34]. In the present study the peak at 532 eV is due to the Oxygen atom from the Rh oxide and the peak at 528 eV is due to the formations of partially reducible Rh^{1+}–CeO_{2-x} compound. Interestingly, the peak due to individual rhodium oxide is more intense in the case of Rh/TiO_2 sample and the peak due to partially reducible Rh–CeO_{2-x} or Rh–TiO_{2-x} is more intense in the case of $Rh/Ce_{0.5}Ti_{0.5}O_2$. These results suggest that the formation of partially reducible Rh–$Ce_{0.5}Ti_{0.5}O_{2-x}$ is higher in the case of $Rh/Ce_{0.5}Ti_{0.5}O_2$ compared to the Rh/TiO_2 sample. This is due to the better reducibility of Ce–Ti mixed oxide compared to the titania alone. XPS results show that the formation of partially reducible oxide is easy in case of $Rh/Ce_{0.5}Ti_{0.5}O_2$ compared to the Rh/TiO_2 catalyst which favors the formation of Rh^{1+} easily.

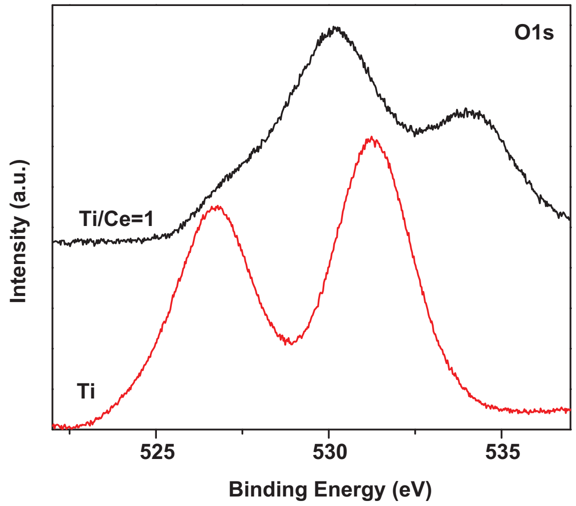

Fig. 12. O1s X-ray photoelectron spectra of activated Rh/TiO_2 and $Rh/Ce_{0.5}Ti_{0.5}O_2$ ((a) Rh/TiO_2 (b) $Rh/Ce_{0.5}Ti_{0.5}O_2$).

Rh 3d X-ray photoelectron spectra of activated Rh/TiO_2 and $Rh/Ce_{0.5}Ti_{0.5}O_2$ catalysts are presented in Fig. 13. Interestingly, both the catalysts exhibit good Rh^{1+}/Rh^0 ratios. This is due to the better interaction between Rh and support and formation of partially reducible oxides during the reduction. Between the Rh/TiO_2 and $Rh/Ce_{0.5}Ti_{0.5}O_2$ samples, $Rh/Ce_{0.5}Ti_{0.5}O_2$ exhibits higher Rh^{1+}/Rh^0 concentrations. This is due to the better reducibility of $Ce_{0.5}Ti_{0.5}O_2$ support compared to the TiO_2 alone, which stabilizes the formation of partially reducible Rh^{1+}–CeO_{2-x} oxide.

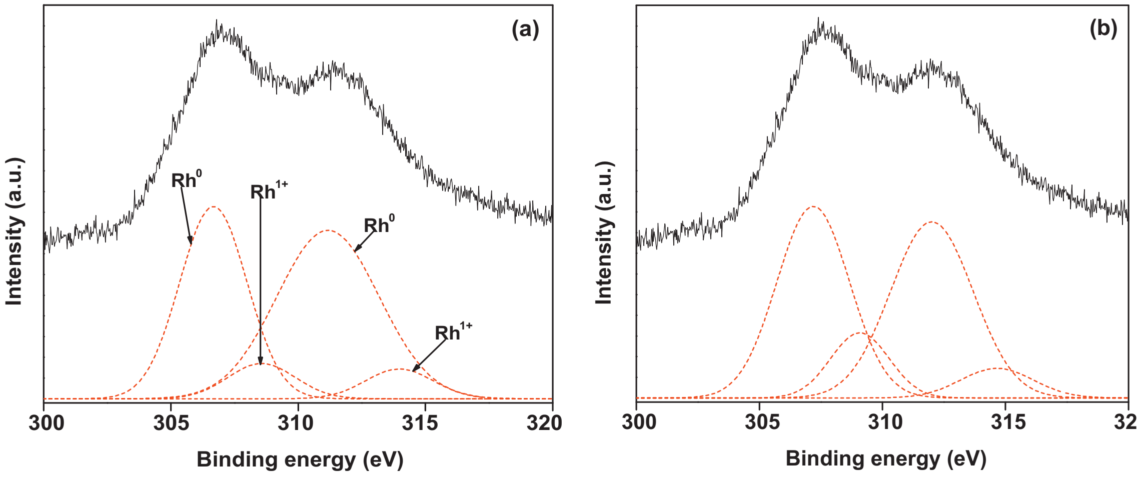

Fig. 13. Rh 3d X-ray photoelectron spectra of activated Rh/TiO_2 and $Rh/Ce_{0.5}Ti_{0.5}O_2$ ((a) Rh/TiO_2 (b) $Rh/Ce_{0.5}Ti_{0.5}O_2$).

Please cite this article in press as: E. Sheerin, et al., Evaluation of $Rh/Ce_xTi_{1-x}O_2$ catalysts for synthesis of oxygenates from syngas using XPS and TPR techniques, Catal. Today (2015), http://dx.doi.org/10.1016/j.cattod.2015.07.050

4. Conclusions

High surface area and high active Rh/$Ce_xTi_{1-x}O_2$ catalysts have been synthesized by eco-friendly coprecipitation and impregnation methods for ethanol synthesis from syngas. The catalytic activity results show that ceria rich based catalysts exhibit better selectivity toward oxygenates and titania rich based catalysts exhibit better selectivity toward hydro carbons. Among the various catalysts Rh/$Ce_{0.75}Ti_{0.25}O_2$ catalyst gives the highest selectivity for oxygenated compound(s). BET surface area of pure supports increases when we go from TiO_2 to $Ce_{0.25}Ti_{0.75}O_2$ catalyst and further increase in the Ce amount leads to a decrease in the surface area. Peaks due to cubic fluorite structure of ceria and anatase titania was observed in X-ray diffraction patterns of the ceria and titania alone. There are no peaks corresponding to either Rh or compounds formation between Rh and support in the in the X-ray diffraction pattern of the Rh based catalysts. Temperature programmed reduction measurements suggest that doping of titanium into the ceria lattice decreases the reduction temperatures of ceria and Rh reduction peaks up to 25% and further increase in the Ti doping into the ceria lattice shift the reduction temperatures toward higher temperature side. X-ray photoelectron measurements show that O 1s peak shifted to higher binding energy side from Ce-rich samples to Ti-rich samples. X-ray photoelectron measurements also show that Rh/$Ce_{0.5}Ti_{0.5}O_2$ exhibits more Rh^{1+} ions compared to Rh/TiO_2 sample. O1s spectra of activated catalysts after pre-reduction also exhibit two peaks one is due to individual oxide and other one is due to Rh^{1+}–CeO_{2-x}.

Dedication to Eli Ruckenstein

In August 1990 I met Professor Eli Ruckenstein and I decided to work with him for my Ph.D. Very soon, I realized that I was working with an exceptional scientist and engineer, somebody who had passion for new findings, a professor who dedicated all his life in trying to understand and study a plethora of very interesting problems. With him I learned how to do research, how to acquire new knowledge and work in numerous catalysis problems and projects at the same time. His life, dedication and appreciation for knowledge was an ideal for me to exemplify throughout my research work and shape my professional attitude for the career I was about to start.

Professor Ruckestein is a leaving legacy and his work and findings will remain always an amazing contribution to benefit our society. I dedicate this paper to him in appreciation of his endless contributions in heterogeneous catalysis and studies of surfaces.

Panagiotis Smirniotis
Chemical Engineering, University of Cincinnati.

Acknowledgements

The authors gratefully acknowledge the financial support from the Ohio Coal Development Authority (Award Number: OCDO-11-12-C-02).

References

[1] N. Kumar, M.L. Smith, J.J. Spivey, J. Catal. 289 (2012) 218–226.
[2] M. Gupta, J.J. Spivey, Catal. Today 147 (2009) 126–132.
[3] C. Maldonado, J.G. Fierro, G. Birke, P. Martinez, J. Chil. Chem. Soc. 55 (2010) 506.
[4] F.J. Keil, Microporous Mesoporous Mater. 29 (1999) 49.
[5] M. Aresta, A. Dibenedetto, A. Angelini, J. CO_2 Util. 3 (2013) 65.
[6] M. Gupta, M.L. Smith, J.J. Spivey, ACS Catal. 1 (2011) 641–656.
[7] C. Riley, AIChE Spring Meeting, Louisiana, New Orleans, 2002.
[8] N.D. Subramanian, G. Balaji, C.S.S.R. Kumar, J.J. Spivey, Catal. Today 147 (2009) 100–106.
[9] J.E. Jackson, F.M. Bertsch, J. Am. Chem. Soc. 112 (1990) 9085.
[10] M. Bjørgen, F. Joensen, M. Spangsberg Holm, U. Olsbye, K.-P. Lillerud, S. Svelle, Appl. Catal. A Gen. 345 (2008) 43.
[11] G.A. Olah, Angew. Chem. Int. Ed. Engl. 44 (2005) 2636.
[12] N.D. Subramanian, J. Gao, X. Mo, J.G. Goodwin Jr., W. Torres, J. Catal. 272 (2010) 204–209.
[13] J.J. Spivey, C. Zhang, C. Liu, W. Xing, Fuel 94 (2012) 401.
[14] M.A. Haider, M.R. Gogate, R.J. Davis, J. Catal. 261 (2009) 9.
[15] X. Sun, G.W. Robert, Appl. Catal. A: Gen. 247 (2003) 133.
[16] M. Pijolat, V. Perrichon, Appl. Catal. 13 (1985) 321.
[17] J.J. Spivey, A. Egbebi, Chem. Soc. Rev. 36 (2007) 1514.
[18] H. Arakawa, T. Fukushima, M. Ichikawa, S. Natsushita, K. Takeuchi, T. Matsuzaki, Y. Sugi, Chem. Lett. (1985), 881.d.
[19] C.M. Li, S.T. Zhang, B.S. Zhang, D. Su, S. He, Y.F. Zhao, J. Liu, F. Wang, M. Wei, D.G. Evans, X. Duan, J. Mater. Chem. 1 (2013) 2461.
[20] I.X. Green, W. Tang, M. Neurock Jr., J.T. Yates, J. Am. Chem. Soc. 134 (2012) 13569.
[21] L.M. Martinez, T.M. Araque, J.C. Vargas, A.C. Roger, Appl. Catal. B: Environ. 132 (2013) 499.
[22] T. Hou, B. Yu, S. Zhang, T. Xu, D. Wang, W. Cai, Catal. Commun. 58 (2015) 137.
[23] A. Cervantes, G. Del Angel, G. Torres, G. Lafaye, J. Barbier Jr., J.N. Beltramini, J.G. Cabañas-Moreno, A. Espinosa de los Monteros, Catal. Today 212 (2013) 2–9.
[24] S.S. Kim, S.J. Lee, S.C. Hong, Chem. Eng. J. 169 (2011) 173–179.
[25] B.M. Reddy, A. Khan, Catal. Surv. Asia 9 (2005) 155.
[26] F. Giordano, A. Trovarelli, C. de Leitenburg, M. Giona, J. Catal. 193 (2000) 273.
[27] J. He, G.K. Reddy, P. Smirniotis, S.W. Thiel, N.G. Pinto, J. Phys. Chem. C 115 (2011) 24300–24309.
[28] B.M. Reddy, K.N. Rao, G.K. Reddy, A. Khan, S.E. Park, J. Phys. Chem. C 111 (2007) 18751–18758.
[29] H.P. Klug, L.E. Alexander, X-ray Diffraction Procedures for Polycrystalline and 748 Amorphous Materials, 2nd ed., Wiley, New York, 1974.
[30] C.D. Wagner, W.M. Riggs, L.E. Davis, J.F. Moulder, in: G.E. Muilenberg (Ed.), Handbook of X-ray Photoelectron Spectroscopy, Perkin-Elmer Corp., Eden Prairie, MN, 1978.
[31] A. Khan, P. Chen, P. Boolchand, P.G. Simrnitios, J. Catal. 253 (2008) 91.
[32] A. Burroughs, A. Hamnett, A.F. Orchard, G. Thornton, J. Chem. Soc. Dalton Trans. 1 (1976) 1686.
[33] B.M. Reddy, K.N. Rao, G.K. Reddy, A. Khan, J. Phys. Chem. C 111 (2007) 18751.
[34] R. Koirala, K.R. Gunugunuri, P.G. Smirniotis, J. Phys. Chem. C 115 (2011) 24084.

Please cite this article in press as: E. Sheerin, et al., Evaluation of Rh/$Ce_xTi_{1-x}O_2$ catalysts for synthesis of oxygenates from syngas using XPS and TPR techniques, Catal. Today (2015), http://dx.doi.org/10.1016/j.cattod.2015.07.050